Journal of Macromolecular Science, Part A
Publication details, including instructions for authors and subscription information:
http://www.informaworld.com/smpp/title~content=t713597274

Novel Synthesis of Polypyrrole Reinforced Nanocomposites and Evaluation of Water Uptake and Blood Compatible Behaviors

Ram Mahloniya[a]; J. Bajpai[a]; A. K. Bajpai[a]
[a] Bose Memorial Research Laboratory, Department of Chemistry, Government Autonomous Science College, Jabalpur, India

Online publication date: 19 November 2010

To cite this Article Mahloniya, Ram , Bajpai, J. and Bajpai, A. K.(2011) 'Novel Synthesis of Polypyrrole Reinforced Nanocomposites and Evaluation of Water Uptake and Blood Compatible Behaviors', Journal of Macromolecular Science, Part A, 48: 1, 9 — 20
To link to this Article: DOI: 10.1080/10601325.2011.528287
URL: http://dx.doi.org/10.1080/10601325.2011.528287

Journal of Macromolecular Science, Part A: Pure and Applied Chemistry (2011) **48**, 9–20

ISSN: 1060-1325 print / 1520-5738 online
DOI: 10.1080/10601325.2011.528287

Taylor & Francis
Taylor & Francis Group

Novel Synthesis of Polypyrrole Reinforced Nanocomposites and Evaluation of Water Uptake and Blood Compatible Behaviors

RAM MAHLONIYA, J. BAJPAI and A.K. BAJPAI*

Bose Memorial Research Laboratory, Department of Chemistry, Government Autonomous Science College, Jabalpur, India

Received, Accepted June 2010

The electrical conductive hydrogels exhibiting *in vitro* blood compatible behavior have been recognized as promising class of materials and have found wide spectrum of applications in biology and technology. In the present investigation, a novel but simple synthetic approach has been evolved that mediates homogeneous impregnation of polypyrrole into a polymer matrix composed of polyvinyl alcohol grafted with copolymer chains of poly(2-acryloamido-2-methyl-1-propanesulphonic acid) (AMPS) and polyacroylonitrile. The prepared electric conductive polymer was characterized by techniques like FTIR, SEM and XRD and, water sorption potential of prepared nanocomposite hydrogel was also evaluated quantitatively. It was revealed by XRD analysis that the impregnation of polypyrrole results in a loss in crystallinity. The size of polypyrrole clusters determined from SEM analysis was found to vary in the range 0.5 to 2 μm. The effect of parameters like composition of the gel, pH, temperature and ionic strength of the swelling bath were also investigated. The prepared nanocomposite was also studied for *in vitro* blood compatibility by performing certain tests such as blood clot formation and percent haemolysis.

Keywords: Nanocomposite, conductive polymer, blood compatibility, swelling

1 Introduction

Conducting polymers (CPs) have electrical and optical properties similar to those of metals and inorganic semiconductors, but also exhibit the attractive properties associated with conventional polymers such as ease of synthesis and processing (1). CPs are the most recent generation of polymers, opening the way to progress in understanding the fundamental chemistry and physics of $\prod$ bonded macromolecules. This unique combination of properties has given these polymers a wide range of applications in the microelectronics industry, including battery technology, photovoltaic devices, light emitting diodes, and electro chromic displays (2), and more recently in the biological fields. Research on CPs for biological applications expanded greatly with the discovery in 1980's that these materials were compatible with many biological molecules such as those used in biosensors. By the mid 1990's CPs were also shown, via electrical stimulation to molecules cellular activities, including cell adhesion, migration, DNA synthesis, and protein secretion (3–6). Specifically, many of these studies involved nerve, bone, muscles and cardiac cells, which respond to electrical impulses. Most CPs present a number of important advantages for biomedical applications, including biocompatibility, ability to entrap and controllably release biological molecules (i.e., reversible doping), ability to transfer charge from a biochemical reaction, and the potential to easily alter the electrical, chemical, physical, and other properties of the CPs to better suit the nature of the specific application. These unique characteristics are useful in many biomedical applications, such as biosensors, tissue-engineering scaffolds, neural probes, drug-delivery devices and bio-actuators. The ability of CPs to scavenge harmful free radicals from the environment has recently been explored as an additional benefit of these materials in biological applications (7). In particular, polymers such as polypyrrole (PPy) and polyaniline (PANI) in their neutral forms were found to react effectively with 2–4 free radicals per monomer unit. This effectiveness of CPs to scavenge free radicals results from their ability to be easily oxidized and therefore does not necessitate electrical stimulation.

The use of conducting polymers in sensors components is a popular research area as such devices can show much higher sensitivities than some conventional systems. Electroactive polymers can change their properties when varying ions and solvents are used in the polymerization

*Address correspondence to: A.K. Bajpai, Bose Memorial Research Laboratory, Department of Chemistry, Government Autonomous Science College, Jabalpur 482001, India. E-mail: akbmrl@yahoo.co.in; akbajpailab@yahoo.co.in

process and this effect can be exploited in ion selective sensors (8).

Development of conductive polymer materials has extended the range of sensor applications to nitrogen oxides detectors (9), a range of organic vapor and gas sensors (10–13) and biosensors (14, 15) Polypyrrole is an especially promising conducting polymer and is positively-charged conjugated. The attractiveness of this polymer for biomedical applications lies in its biocompatibility, ease of preparation, stability in air, and its ability to incorporate a wide variety of dopant ions. Apart from its electron-conducting properties, this polymer also possesses the so-called intercalation property, whereby entrapped counter ions can be electrically released and incorporated when electrically activated. This is accompanied by a change in volume, thus making polypyrrole an attractive candidate for artificial muscles and drug delivery substrates. Polypyrrole can often be used to produce reliable and accurate sensors, due to its high environmental stability; it can also be made sensitive to a wide variety of chemical species.

Conducting polymers such as polypyrrole have a long history of use as polymer actuators (16), and biomedicine, most notably as neural interfaces and scaffolds for neural tissue growth. They have also been considered as candidates for "wearable" sensors and interfaces for biosensors and DNA chips. Reza Ansari (17) developed the polypyrrole conducting polymers for the use in electronics industry by loading of conductive powders such as silver, gold and graphite (sometimes as high 80% by weight) with the polymer matrix. PPy is used in magnetic nanoparticles (MN), which have recently gained broad interest in various fields, such as medicine, biomedicine (18–22), in the construction of loudspeakers (23–24), as sealing materials (25–30) and sink float separation (31–34).For many medical and biomedical applications, it is essential to functionalize their surfaces. The functional groups can be directly attached to the magnetic nanoparticles by adsorption or by using polymers, such as polypyrrole (PPy). The PPy polymer was found to be biocompatible *in vitro* and *in vivo* (35, 36). Turcu et al. (37) reported the synthesis and characterization of the nanocomposites obtained by combining polypyrrole (PPy) and magnetic nanoparticles Fe_3O_4. *In situ* polymerization of pyrrole was carried out by Murugendrappa et al. (38) in the presence of fly ash to synthesize polypyrrole–fly ash composites by the chemical oxidation method. Rajagopalan et al. (39) described a polypyrrole–based strain sensor dedocated to measure bladder volume in patients with urinary dysfunction. Gomez et al. (40) studied the effect of the electrical stimulation on PPy with an immobilized nerve growth factor on its surface linked with a layer of polyallylamines conjugated to an arylazido functional group. Gomez et al. (41) reported that embryonic hippocampal neurons increase the number of cells by two fold when cultured on electro polymerized PPy on Indium tin oxide, patterned with 1 and 2 μm wide channels using e-beam lithography. In all the applications of PPy conducting nanostructure materials, the homogeneous deposition of PPy within the host polymer matrix is the key controlling factor. Thus, realizing the significance of the PPy containing polymers and composites in biology and medicine, an attempt has been made to design and develop homogeneously impregnated PPy nanocomposites of polyvinyl based nanocomposites and investigate their water sorption and blood compatible behavior.

2 Experimental

2.1 Materials

Polyvinyl alcohol (PVA) (98.6% hydrolyzed) was obtained from the Research Lab, Mumbai, India and used as received. 2-Acryloamido-2-methyl-1-propanesulphonic acid (AMPS) was purchased from Aldrich (Germany). Pyrrole, and acrylonitrile (AN) were purchased from Merck Ltd. (Mumbai, India) and later was purified by distillation at 55°C. Other chemicals such as ammonium persulphate (APS), potassium persulphate (KPS) were also of analytical grade and used without any further purification.

2.2 Methods

2.2.1. *Preparation of Gel*

A polymer matrix composed of PVA–g-P (AMPS-co-AN) was prepared by using KPS as polymerization initiator. In a typical experiment, 2 g PVA was dissolved in 20 mL of hot double distilled water and to this solution were added precalculated amounts of AMPS (7.23 mM), AN (30.38 mM), KPS ($11.10 \cdot 10^{-2}$ mM). The entire reaction mixture was homogenized and kept in a Petri dish (Corning glass, 25″ diameter) maintained at 35 ± 0.2°C for 24 h. After the reaction was complete, the entire mass was converted into a semi-transparent film and it was purified by equilibrating it in doubled distilled water for a week. This swollen gel was dried at room temperature, cut into rectangular pieces and stored in airtight plastic bags.

2.2.2. *Impregnation of Polypyrrole*

The required quantity of pyrrole (2.73 mM) was dissolved in 3 mL of distilled water and the gel prepared was allowed to soak in the pyrrole solution for 24 h. The pyrrole containing swollen gel was dried and then again left in a 0.3 M APS solution to soak the required quantity of APS from the solution. As soon as the APS enters into the polymer matrix the APS initiates polymerization of pyrrole. As the polymerization progresses, the semi-transparent gel readily turns black. After the polymerization is over, the PPy impregnated gel is repeatedly washed with distilled water and allowed to dry at 30 ± 0.2°C. for 24 h. The whole scheme

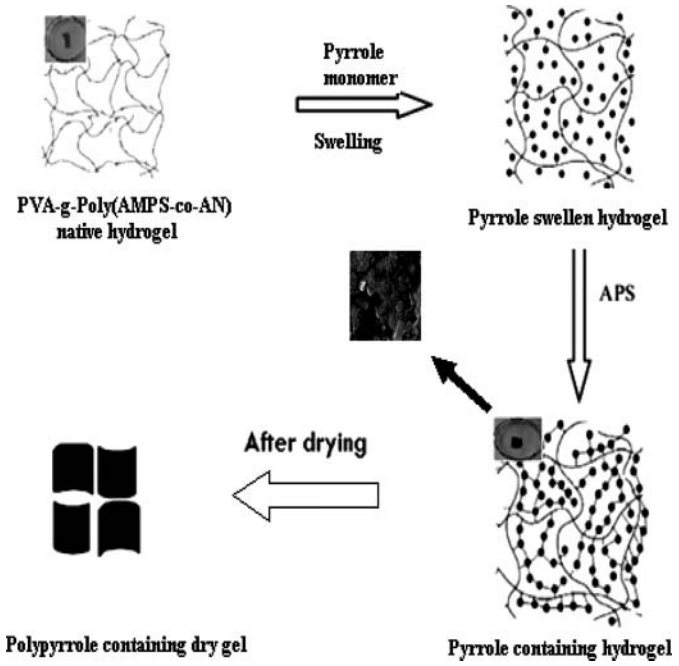

Fig. 1. Schematic presentation of preparation of Polypyrrole containing nanocomposite of polyvinyl alcohol based hydrogel.

of preparation of nanocomposite hydrogel is shown in Figure 1.

The percentage of impregnation of PPy into gel was calculated by using the equation:

$$\%\ \text{Impregnation} = \frac{(W_{PPy} - W_{DRY}) * 100}{W_{DRY}} \qquad (1)$$

where W_{PPy} is the weight of dry PPy impregnated gel and W_{Dry} is the initial weight of polymer gel.

2.3 Characterization

2.3.1. *FTIR Spectral Analysis*

To gain insights into the structural information of prepared PPy impregnated gel, the FTIR spectra of PPy powder, polymer hydrogel and PPy impregnated matrix were recorded on a FTIR spectrophotometer (Perkin-Elmer, 1000 Paragon). For recording FTIR spectra of native and PPy impregnated films, quite thin and transparent samples were prepared by a solution casting method and the prepared films were directly mounted on a spectrophotometer to be scanned in the range 4000–500 cm^{-1}.

2.3.2. *XRD*

In order to gain information about the crystalline nature of the prepared native and PPy impregnated gels, the X-ray diffraction spectra were recorded (on an XRD apparatus). The dried gels were placed on the glass slide specimen holder and exposed to X-ray in a vertical goniometer assembly.

2.3.3. *SEM*

The SEM of native and PPy impregnated gels were recorded on a scanning electron microscope (Philips 515) for their morphological characterization.

2.4 Water Uptake Measurements

A conventional gravimetric procedure (42) was followed for monitoring progress of the water uptake process. In brief, a pre-weighed dry piece of nanocomposite gel was immersed into distilled water at a definite temperature, taken out at predetermined time intervals, gently pressed between two filter papers to remove excess water and finally weighed on a sensitive balance (APX-203, Denver, Germany). The degree of water sorption was quantified in terms of the swelling ratio as calculated below:

$$\text{Swelling ratio} = \frac{Ws}{Wd} \qquad (2)$$

where W_s and W_d are the swollen and dry weights of the gels, respectively.

2.5 *In Vitro* Blood Compatibility

The *in vitro* blood compatibility of the prepared hydrogels was determined by the methods described as below.

2.5.1. *Clot Formation Test*

The anti-thrombogenic potential of the hydrogel surface was judged by the blood clot formation test, as described elsewhere (43). In brief, the specimens were equilibrated with saline water (0.9% w/v NaCl) at 37°C for 24 h. and to these swollen samples were added 0.5 mL of ACD blood and 0.03 mL of $CaCl_2$ solution (4 mol L^{-1}) to start the thrombus formation. 4.0 mL of deionized water was added to stop the reaction and the thrombus formed was separated by soaking in water for 10 min at room temperature and then fixed in a 36% formaldehyde solution (2.0 mL) for another 10 min. The fixed clot was placed in water for 10 min and after drying, its weight was recorded. The same procedure was repeated for glass surface, blood bags and for the gels of varying compositions and respective weights of thrombus formed was recorded.

2.5.2. *%Haemolysis Tests*

Haemolysis experiments were performed on the surfaces of the prepared hydrogels following a method described elsewhere (44). In a typical experiment, a dry gel piece (4 cm^2) was equilibrated in normal saline water (0.9% w/v NaCl) at 37°C for 24 h and human ACD blood (0.25 mL) was added into the gels. After 20 min, 2.0 mL of saline water was added into the specimens to stop haemolysis and the sample was incubated for 60 min at 37°C. Positive and negative controls were obtained by adding 0.25 mL of human ACD blood and 0.9% NaCl solution, respectively to 2.0 mL of bi-distilled water. Incubated

samples were centrifuged for 45 min, the supernatant was taken and its absorbance was recorded at 545 nm. The percentage haemolysis was calculated using the following relationship.

$$\text{Haemolysis (\%)} = \frac{A_{\text{test-sample}} - A_{(-)\text{Control}}}{A_{(+)\text{control}} - A_{(-)\text{Control}}} \times 100. \quad (3)$$

where A is absorbance. The absorbance of positive and negative controls was found to be 1.73 and 0.048, respectively.

3 Results and Discussion

3.1 FTIR Spectra

Figures 2 (a) and (b) represent FTIR spectra of PVA and PAVA-g-P(AMPS-co-AN) polymer films, respectively scanned in the range 400–4000 cm^{-1}. The peaks observed at 1244, 1683, and 2976 cm^{-1} are due to the SO_3H, CO, and CONH groups in stretching mode, respectively of PAMPS which appears in the spectra of grafted gel only, i.e., PVA-g-P(AMPS-co-AN) (Fig. 2b).This obviously confirms the grafting reaction. The characteristic peaks at 3621 cm^{-1} suggests for the presence of hydrated -OH and a minor peak at 2976 cm^{-1} implies for C-H stretching of methylene group of constituent vinyl polymers. The spectra also contain a sharp peak at 2359 cm^{-1} which is due to CN stretching of nitrile group of polymer. Figure 2 (c) and (d) represent the FTIR spectra of PPy powder and PPy impregnated PVA-g-P (AMPS –co-AN) gel film respectively. The characteristic peaks in Figure 2 (c) at 923, 1047, 1400 and 3100 cm^{-1} confirm the presence of PPy (45). The spectra 2 (d) of PPy impregnated PVA-g-P(AMPS-co-AN) gel film contain peaks at 686, 1168, 1249, and 1600 cm^{-1} indicating

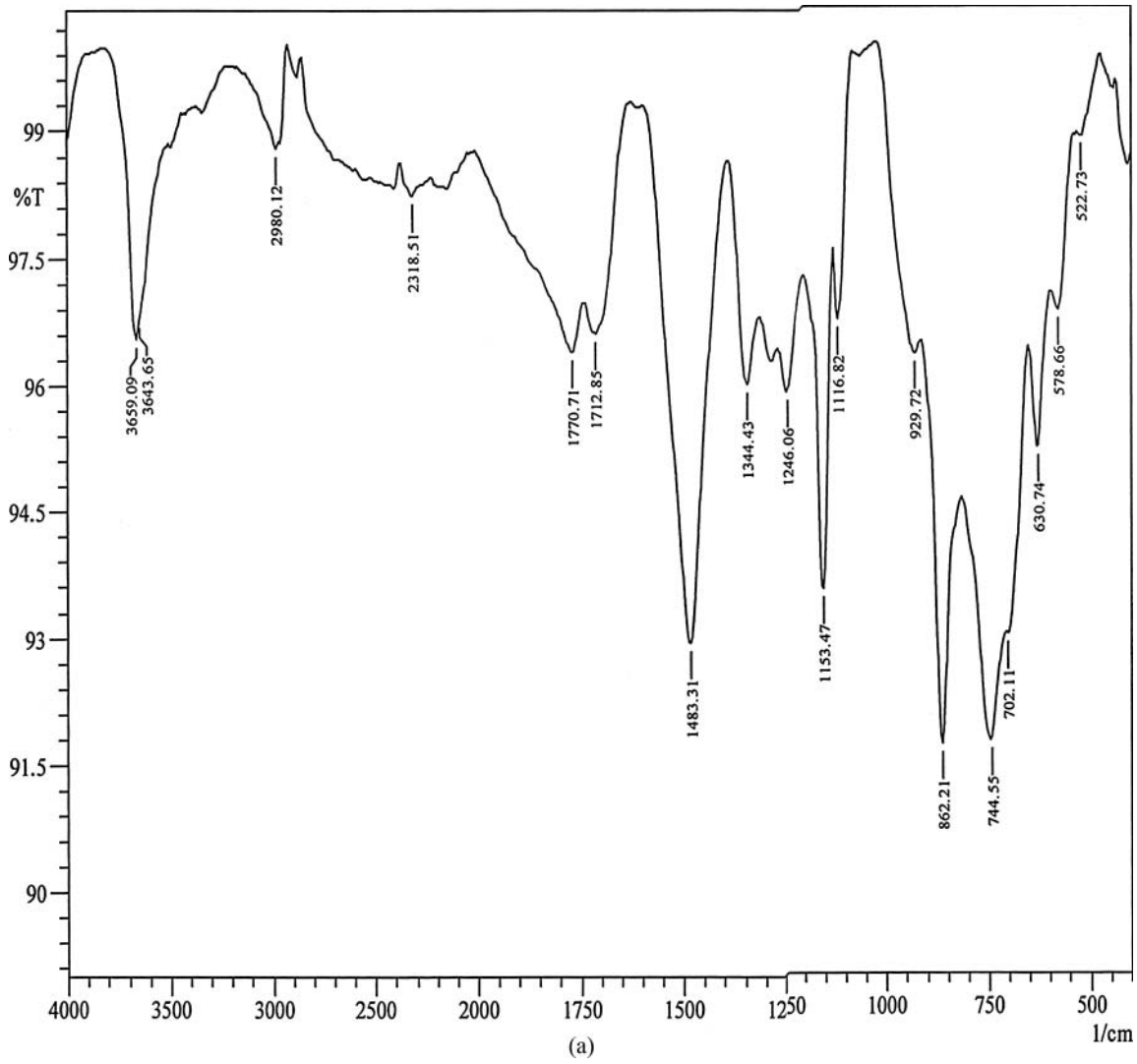

Fig. 2. FTIR Spectra of (a) PVA (b) native PVA-g-P (AMPS-co-AN) gel, (c) PPy powder and (d) PPy-impregnated gel.

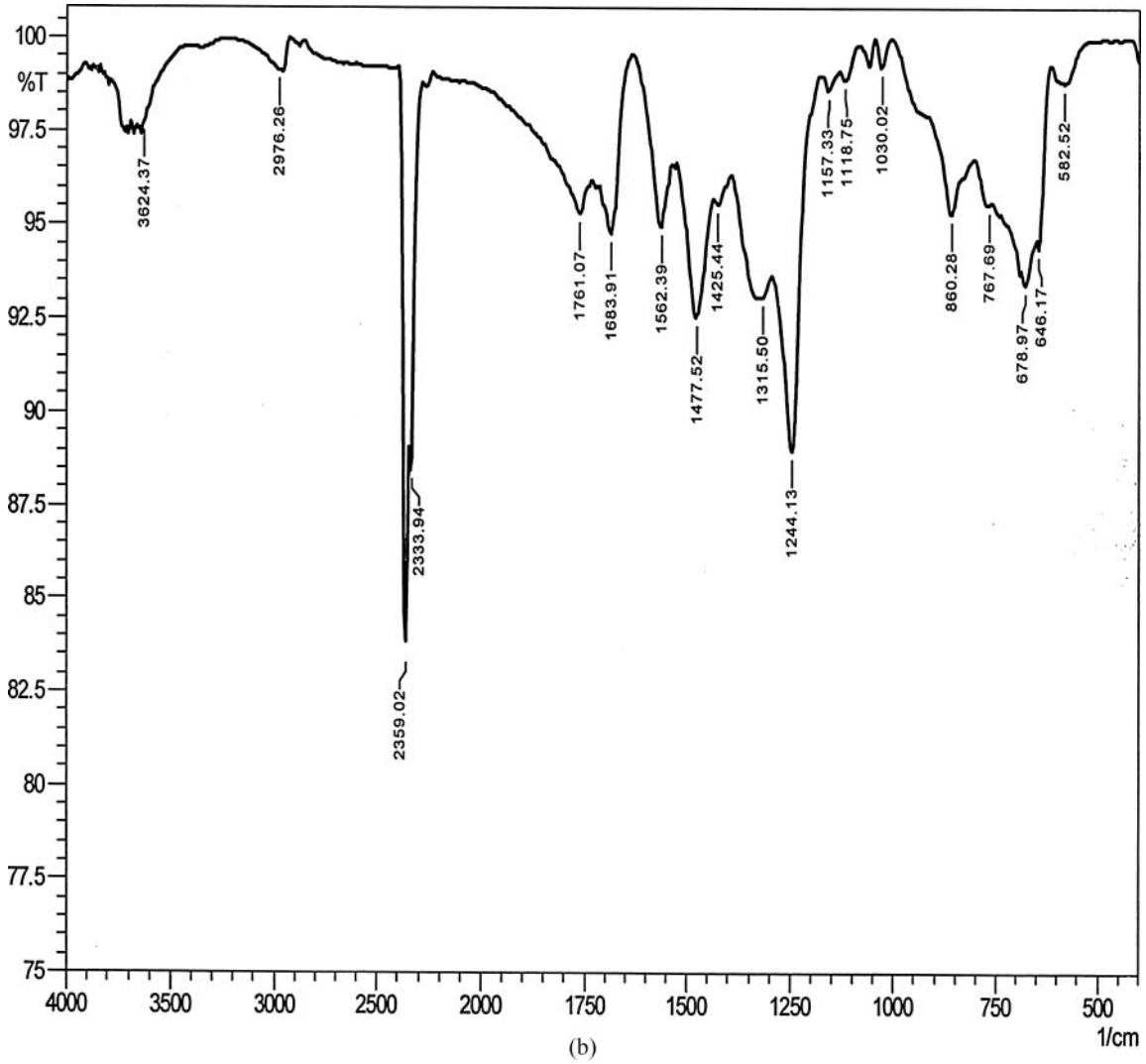

Fig. 2. (Continued).

the presence of aromatic C-H, aromatic amide, and aromatic C-C stretching which confirm the impregnation of PPy into the polymer nanocomposite gel.

3.2 X-Ray Diffraction Analysis

The XRD patterns of the prepared native and PPy–impregnated gels are shown in Figure 3(a) and (b), respectively. Figure 3(a) shows a prominent peak near 20.8° which is characteristic of the PVA. Other minor peaks appeared around 39.1° and 41.70 could be attributed to crystallites of grafted poly(2-acrylonitrile-2-methyl-1-propanesulphonic acid) (PAMPS) chains. The diffraction pattern of PPy–impregnated gel is shown as spectra 3(b), which not only exhibits a characteristic peak near 19.9° (due to PVA) but also at 24.10, indicative of characteristic peaks of PPy. Thus, XRD patterns of impregnated gel provide additional evidence of PPy formation within the polymer matrix. A comparison of the peak area of the two diffractograms clearly indicates that upon PPy impregnation, the polymer matrix loses its crystallinity as is evident from the increase in broadness of the XRD spectra (b). The loss in crystallinity due to PPy impregnation may be explained by the fact that because of *in situ* polymerization of pyrrole within the matrix, the PPy chains produced due to polymerization may bring disorder in the chains packing and, therefore, may result in loss of crystallinity.

Crystallinity % (1) native peak (a) 17%, (b) 36%
(2) PPy impregnated peak (a) 10%, (b) 15

3.3 SEM Analysis

The morphological features of the prepared native and PPY-impregnated composite films have been studied by recording SEM images of the films as shown in Figure 4(a)

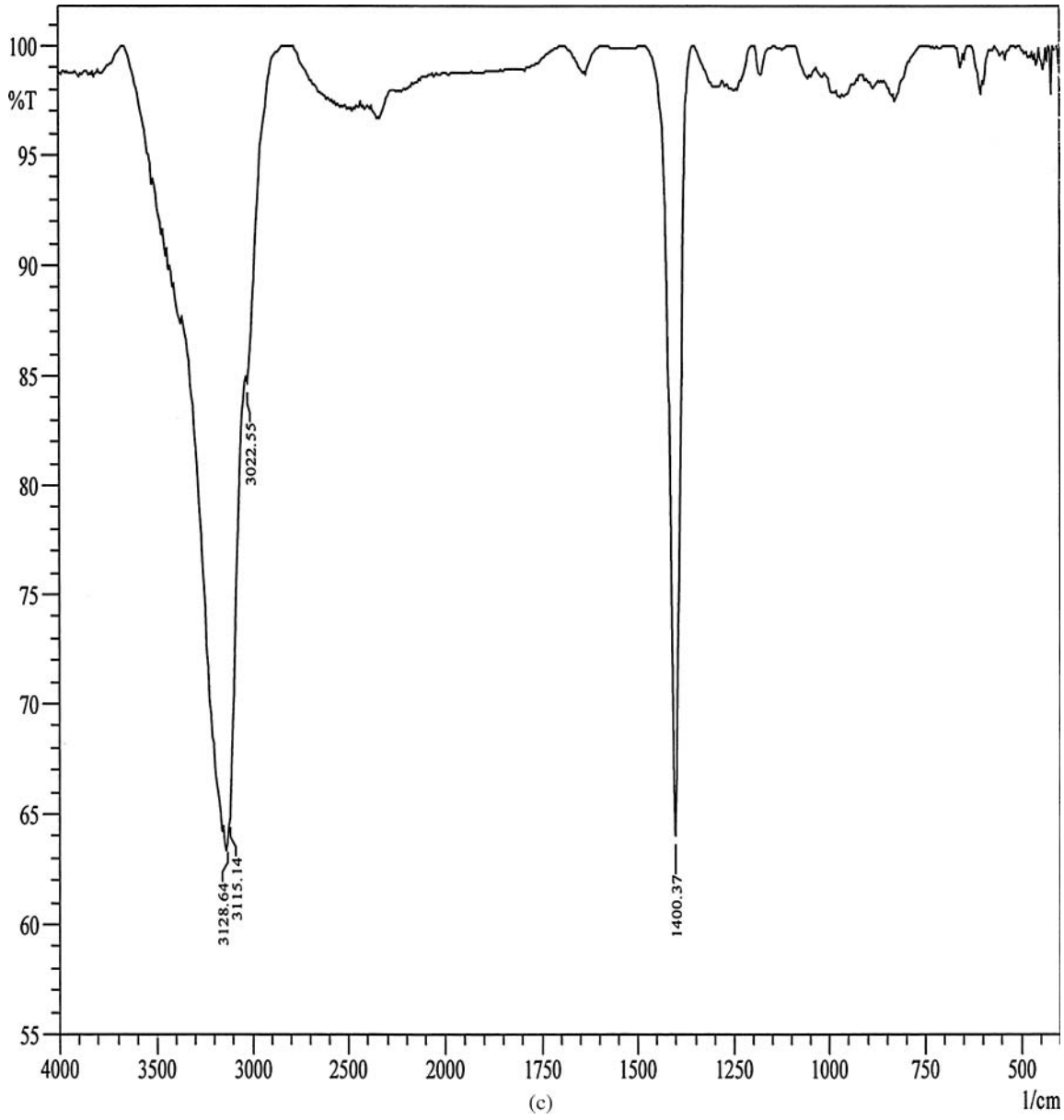

Fig. 2. (Continued).

and (b), respectively. It is clear from the image (a) that the surface of the native gel is quite homogeneous and shows no cracks, voids or unevenness. This suggests that after grafting of PAMPS and PAN chains onto PVA backbone, the matrix remains homogeneous in composition suggesting that the polymer components are compatible. However, impregnation of PPy into the matrix develops heterogeneity in the matrix as is evident from the SEM image (b). It is clear from the image (b) that impregnated PPy molecules from clusters like morphology varying in the sizes 0.5 to 2 μm. The formation of PPy clusters within the polymer matrix could be attributed to hydrophobic nature of the PPy molecules which may aggregate due to hydrophobic dispersion forces.

3.4 Water Sorption Measurements

3.4.1. *Effect of PVA*

The influence of increasing concentration of PVA on the degree of water sorption was investigated by varying the amount of PVA in the range 1–5 g in the feed mixture of the hydrogel. The results are shown in Figure 5, which clearly indicate that the swelling ratio decreases with the increasing amount of PVA. The observed results may be explained by the fact that with an increase in PVA concentration, the volume fraction of polymer in the hydrogel increases, which enhances the degree of interaction between the PVA–PVA and PVA–AMPS molecules. Thus, an increased extent of crosslinking in the hydrogel results in a

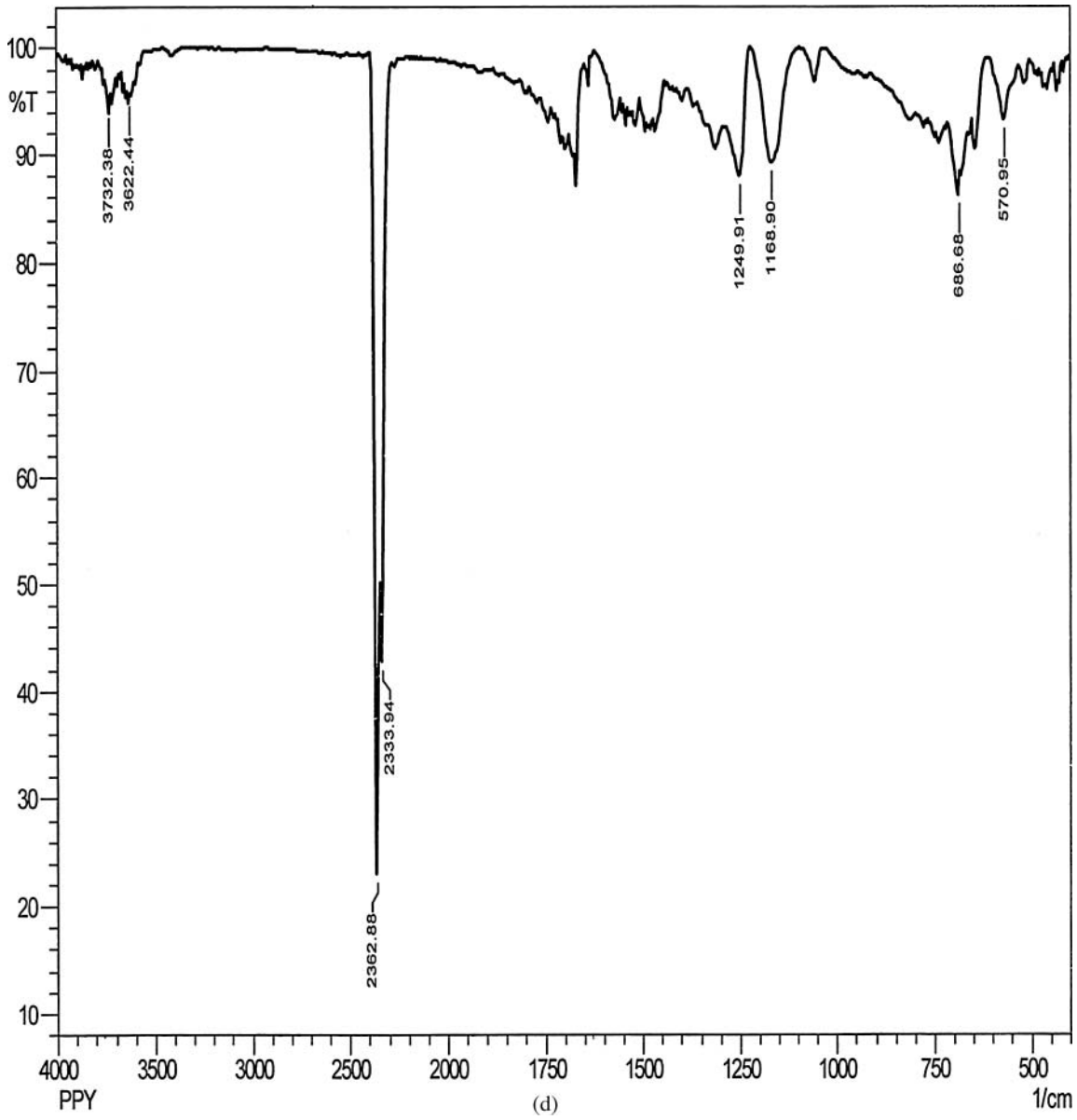

Fig. 2. (Continued).

fall in the swelling ratio. The observed results may also be attributed to the fact that since PVA itself has a tendency to form reversible gel and the increasing amount of PVA results in a large number of crystallites formed.

3.4.2. *Effect of Acrylonitrile*

In order to investigate the influence of AN content in the hydrogel on its swelling behavior the concentration of acrylonitrile (AN) was varied in the polymer mixture in the range 15.19 to 60.76 mM. The results are shown in Figure 6 which clearly reveal that the swelling ratio constantly increases when concentration of AN is increased in the range 15.19 mM to 60.76 mM. The noticed increase in water uptake may be explained by the fact that because of the hydrophobic nature of the polyacroylonitrile, its increasing amount in the hydrogel results in an enhanced pore sizes in the hydrogel, which allow a larger amount of water.

3.4.3. *Effect of (Monomer) AMPS*

In order to study the influence of AMPS variation on the swelling ratio of the hydrogel, the concentration of AMPS was varied in the range 2.41 to 9.64 mM while keeping concentrations of other constituent as constant. The results are shown in Figure 7 which show that an increase in concentration of AMPS results in an increased swelling ratio. The results may be explained by the fact that increased AMPS concentration results in an increased grafting of PAMPS chains onto PVA molecule which subsequently enhances

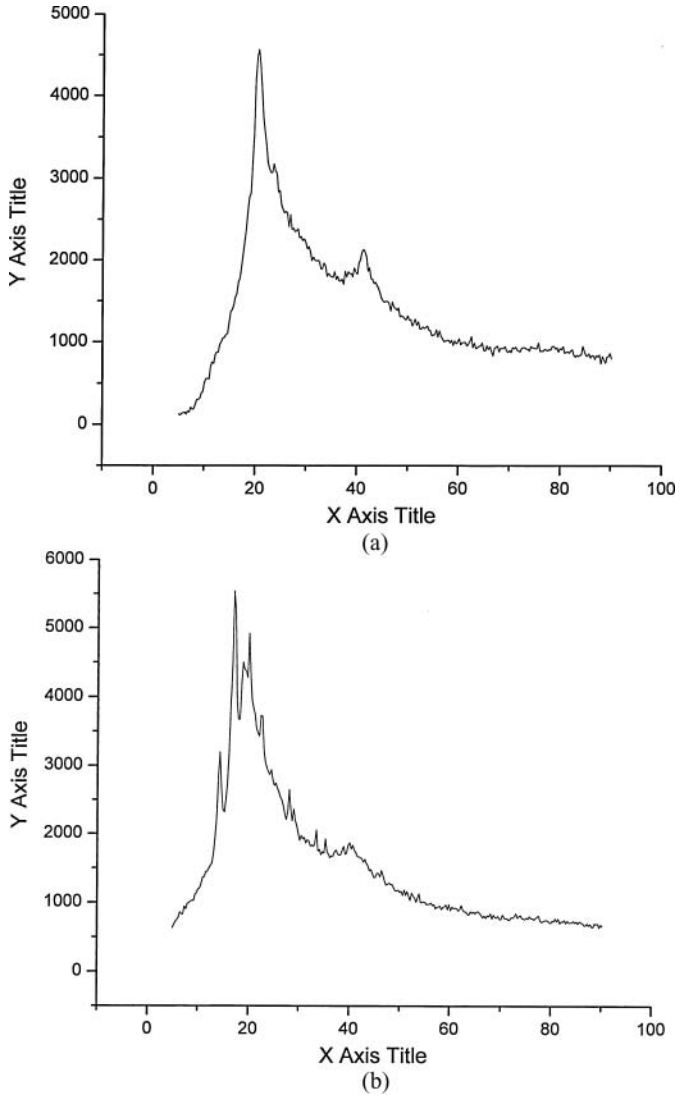

Fig. 3. XRD spectra of (a) native PVA-g-P (AMPS-co-AN) gel, and (b) PPy-impregnated gel.

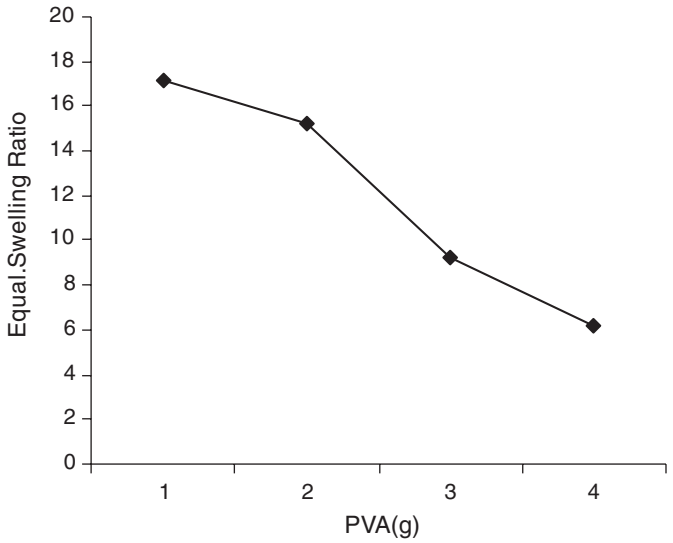

Fig. 5. Effect of varying amounts of PVA on swelling ratio of definite composition [AN] = 60.76 mM, [AMPS] = 7.23 mM.

electrostatic repulsion among the charged centers of PAMPS chains, thus clearly widening the pore sizes of the polymer networks. This leads to an increased swelling. Another reason for the observed increase in swelling ratio could be that with an increase in monomer concentration the molecular weight of the polymer chains in the hydrogel network also increases, which results in formation of a larger mesh sized network and therefore leads to greater water sorption.

3.4.4. *Effect of pH*

pH Responsive hydrogels constitute an important class of biomaterials, and play a significant role in formulating targeted drug delivery systems (46). The underlying principle for targeted drug delivery is the pH controlled swelling of

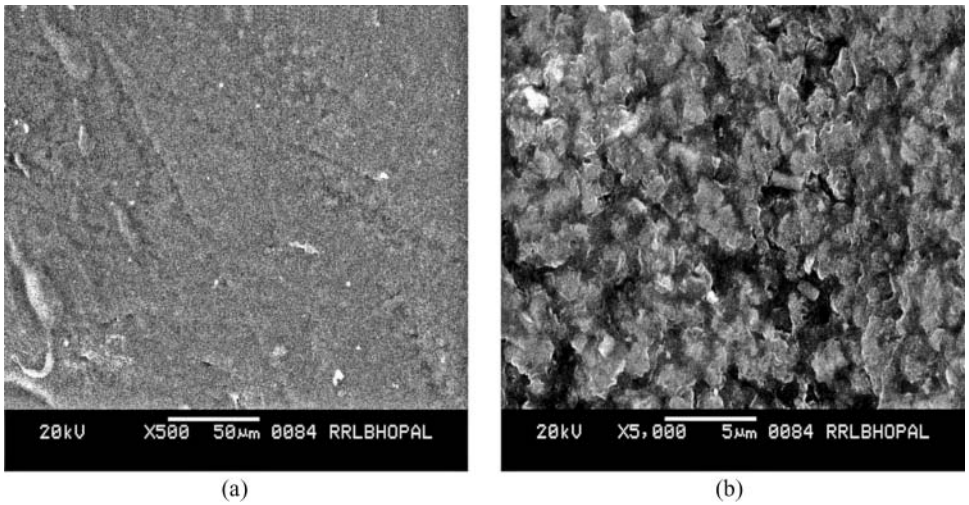

Fig. 4. SEM images of (a) native PVA-g-P (AMPS-co-AN) gel, and (b) PPy-impregnated gel.

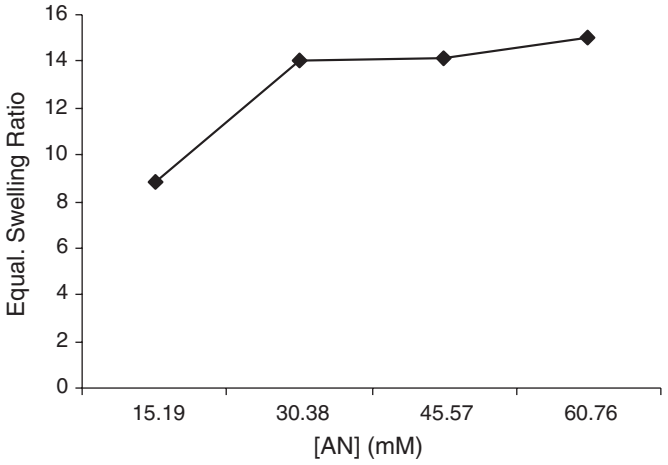

Fig. 6. Effect of varying amounts of AN on swelling ratio of definite composition [PVA] 3 g, [AMPS] = 7.23 mM.

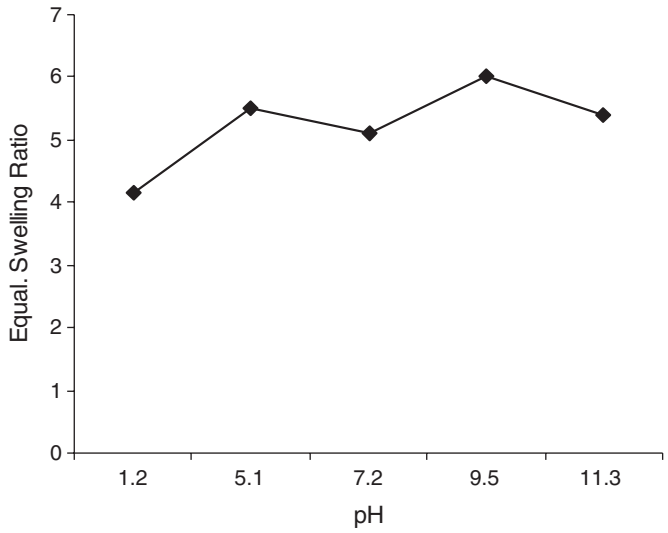

Fig. 8. Effect of pH on Swelling ratio of hydrogel of definite composition [PVA] = 3 g, [AMPS] = 7.23 mM, [AN] = 60.76 mM.

hydrogel which normally results from the change in relaxation rate of network chains with changing pH of the swelling medium. The effect of pH on the swelling ratio of the hydrogel has been studied by varying the pH of the swelling medium in the range 1.2.to11.3. The results are shown in Figure 8, which clearly reveals that the swelling ratio of the hydrogel increases up to pH 9.5 and thus achieves an optimum swelling and, thereafter, decreases with a further increase in the pH. The results can be explained by the fact that with increasing pH of the medium, the sulphonic acid groups of AMPS are ionized and generate sulphonate ions along the macromolecular chains which, because of mutual repulsion, facilitate the chain relaxation and cause greater swelling. The decrease observed in the swelling ratio after pH 9.5 could possibly be due to net negative charges on polymeric chains, which cause electrostatic repulsion resulting in unfolding of macromolecules which again cause a fall in water sorption capacity.

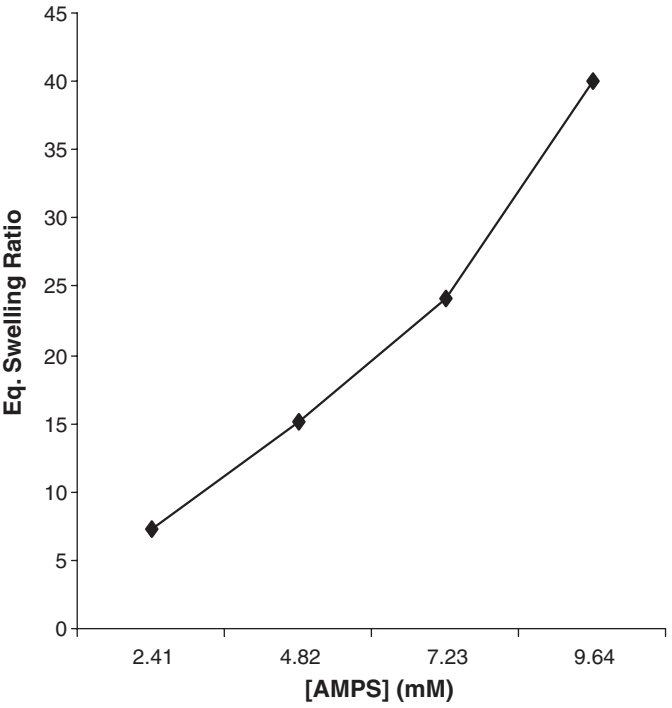

Fig. 7. Effect of varying amounts of AMPS on swelling ratio of definite composition [PVA] = 3 g, [AN] = 60.76 mM.

3.4.5. *Effect of Temperature*

In the present study, the effect of temperature on the swelling ratio of the nanocomposite gel has been investigated by varying the temperature of the swelling medium in the range 15–45°C. The results are depicted in Figure 9, which reveal that the swelling ratio increases with increasing temperature of the swelling medium. The results can be explained by the fact that temperature has a direct influence on the swelling behavior of a hydrogel as it affects both the segmental mobility of the hydrogel chains, as well as the diffusion of penetrate water molecules, into the gel matrix. Thus, with increasing temperature, the network chains also undergo faster relaxation due to increased kinetic energy and facilitate water sorption process.

3.4.6. *Effect of Salts*

The influence of the presence of salts in the swelling medium of a hydrogel is of importance in agriculture and biomedical applications, for example, as water reservoirs in agriculture, and for hydrogels as implants (47) for drug release applications. In principle, change in the swelling behavior due to presence of salts can affect the mechanical properties of the material as well as the 'tortuosity' of the matrix which gives rise to different diffusion coefficients of drug release (48). The effect of salts on the swelling ratio was studied by

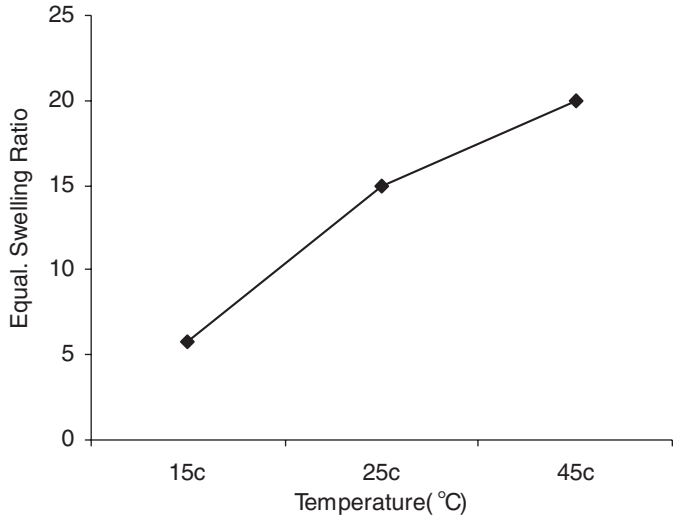

Fig. 9. Effect of temperature on Swelling ratio of hydrogel of definite composition [PVA] = 3 g, [AMPS] = 7.23 mM, [AN] = 60.76 mM.

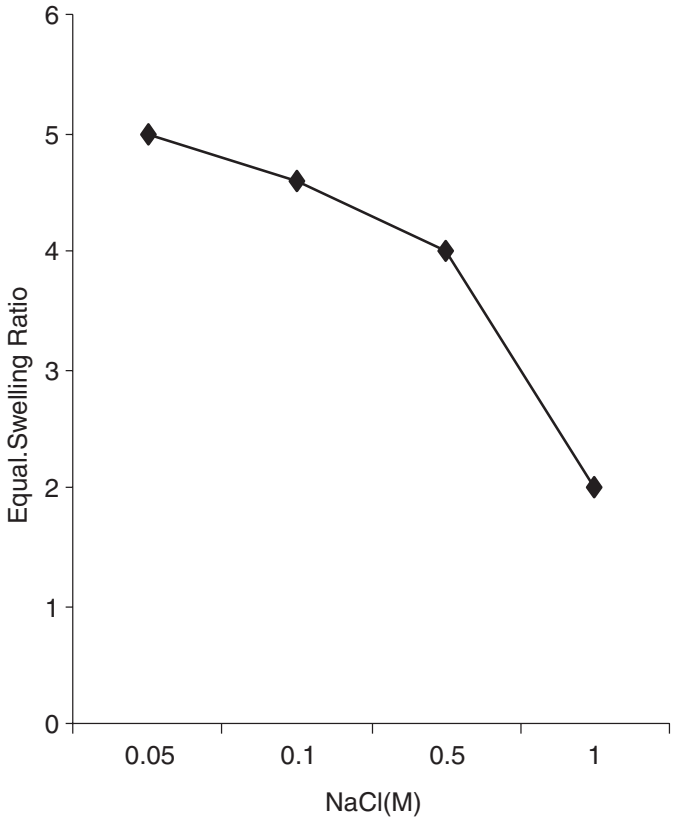

Fig. 10. Effect of salts on Swelling ratio of hydrogel of definite composition [PVA] = 3 g, [AMPS] = 7.23 mM, [AN] = 60.76 mM.

adding NaCl in the concentration range 0.05–1 M to the swelling medium. The results are presented in Figure 10, which clearly reveal that the swelling ratio decreases with increasing salt concentration in the swelling medium. The results may be explained by the fact that with increasing salt concentration, the osmotic pressure decreases due to a decrease in the concentration difference between mobile ions in the exterior and interior of the swelling hydrogel and, consequently the swelling ratio decreases.

3.5 Evaluation of Biocompatibility

The selection of a material to be employed as a biomaterial for a specific end use must meet several criteria such as physicochemical properties, functions desired, nature of the physiological environment, adverse effects in the case of failure, expected durability and consideration relating to cost and ease of production. Whatever may the type of materials, the biocompatibility is the foremost requirement for all biomaterials. In the present study, the assessment of biocompatibility has been made on the basis of two *in vitro* tests viz. blood-clot formation and haemolysis assay as discussed below.

3.5.1. *Blood Clot Formation*

For many biomedical applications, it is desirable to have a high anti-thrombogenic potential of the biomaterial

Table 1. Biocompatibility parameters with varying composition of hydrogels

S.N.	*PVA (g)*	*AMPS (mM)*	*AN (mM)*	*Ppy (%)*	*Blood Clot (g)*	*Haemolysis (%)*
1	2	4.82	30.38	nil	nil	90.19
2	3	4.82	30.38	nil	0.0035	88.19
3	4	4.82	30.38	nil	0.0005	50.12
4	3	2.41	30.38	nil	nil	70.84
5	3	4.82	30.38	nil	0.0001	64.81
6	3	7.32	30.38	nil	0.0036	45.54
7	3	4.82	15.19	nil	0.0065	73.73
8	3	4.82	46.57	nil	0.0028	60.6
9	3	4.82	60.76	nil	0.0009	55.42
10	3	4.82	60.76	2	nil	85
11	3	4.82	60.76	8	nil	90
12	3	4.82	60.76	11	nil	96

implanted into the body for some specific purpose. In the present investigation, the anti-thrombogenic property of the hydrogel has been judged by monitoring the amount of blood clot formed by blood clot formation test. The results are summarized in Table 1, which clearly indicate that the amount of the blood clot constantly decreases with increasing amount of PPy in the hydrogel. The results may be explained on the basis of the fact that PPy is a hydrophobic polymer and, therefore, is not expected to provoke either any damage of blood cells or any change in the structure of plasma proteins. This clearly results in antithrombogenic nature of the hydrogel surface.

3.5.2. *Haemolysis Test*

In the present study, the nanocomposite hydrogels were also tested for hemolytic activity. The results are summarized in Table 1, which clearly indicate that on increasing the concentration of PPy in the feed mixture of hydrogel, the haemolysis constantly decreases. The observed results are due to the reason that with changing PVA, AMPS, AN and PPy the surface becomes more blood compatible due to the hydrophilic nature of the PVA, AMPS and hydrophobic nature of AN and PPy. The results are consistent with the clot-formation results.

4 Conclusions

The copolymerization of ionic monomers AMPS and AN in the immediate presence of PVA and crosslinking agent MBA results in formation of a graft copolymer in which PVA macromolecule has been grafted by macromolecular chains of P(AMPS-co-AN). The resulting native grafted copolymer imbibes pyrrole and upon free radical polymerization yields a dark film of polypyrrole impregnated graft copolymer matrix.

The FTIR analysis of the film not only confirms the occurrence of graft copolymerization reaction but also the presence of functional groups of the constituent monomers. The XRD analysis suggests that the impregnation of polypyrrole into the polymer matrix brings about a drop in the percent crystallinity. The morphological characterization of the nanocomposite gel indicates that the polypyrrole macromolecules are present in the cluster forms varying in sizes between 0.5 to 2 μm.

The water uptake capacity of the nanocomposite is found to vary significantly with the composition of the matrix, as well as with the experimental conditions. It is noticed that the swelling ration decreases from 18 to 7% when the amount of PVA increases from 1.0 to 4.0 g. Likewise, the swelling ration increases significantly when the concentrations of the monomers, AMPS and AN, increase from 2.41 to 9.64 mM and 15.19 to 60.76 mM, respectively.

The pH of the swelling bath also influences swelling behavior of the nanocomposite gel. When the pH increases from 1.2 to 9.5, the swelling ratio increases whereas beyond further increase beyond 9.5, the swelling decreases. On the contrary, the swelling ratio is found to increase continuously when temperature of the swelling medium increases from 15 to 45°C.

The swelling is also affected by the presence of salts as is evident from the results of salt effect. When the concentration of NaCl increases from 0.05 to 1.0 M, the water sorption capacity constantly decreases.

The prepared native and polypyrrole impregnated gels are found to show *in vitro* blood compatible behavior. It is found that whereas the native gel shows relatively higher antithrombogenic nature, the impregnation of polypyrrole results in a significantly higher increase in antithrombogenic nature of the matrix.

References

1. Heeger, A.J. (2002) *Synth. Met*., 125, 23–42.
2. Gurunathan, K., Murugan, A.V., Marimuthu, R., Mulik, D.P. and Amalnerkar, U.P. (1999) *Mater. Chem. Phys.*, 61,173–91.
3. Foulds, N.C. and Lowe, C.R. (1986) *J. Chem. Soc. Faraday Trans.*, 82, 1259–64.
4. Umana, M. and Waller, J. (1986) *Anal. Chem.*, 58, 2979–83.
5. Wong, J.Y., Langer, R. and Ingber, D.E. (1994) *Proc Natl. Acad. Sci. USA.*, 91, 3201–04.
6. Shi, G., Rouabhia, M., Wang, Z., Dao, L.H. and Zhang, Z. (2004) *Biomaterial*., 25, 2477–88.
7. Nikolaidis, M.G., Sjdic, J.T., Bowmaker, G.A., Cooney, R.P. and Kilmartin, P.A. (2004) *Synth. Met.*, 140, 225–32.
8. Roncali, J. (1992) *Chem. Rev.*, 92, 711–38.
9. Waltman, R.J. and Bargon, J. (1984) *Tetrahedron,* 40, 3963–70.
10. Walton, D.J., Iniesta, J., Platter, M., Mason, T.J., Lorimer, J.P., Ryley, S., Phull, S.S., Chyla, A., Heptinstall, J., Thiemann, T., Fuji, H., Mataka, S.Y. and Tanaka, Y. (2003) *Ulterason. Sonochem.*, 10, 209–16.
11. Hotta, S., Hosaka, T. and Shimotsuma, W. (1983) *Synth. Met.*, 6, 319–20.
12. Diaz, A. F. and Bargon, J. *In Handbook of Conducting Polymers.* (Skotheim, T.J., Ed.) Marcel Dekker: New York, 1, 81, 1986.
13. Jansson, R., Armin, M., Bjorklund, R. and Lundstrom, I. (1985) *Thin Solid Films*, 125, 205–211.
14. Hillman, A.R. and Mallen, E.F. (1987) *J. Electroanal. Chem.*, 220, 351–67.
15. Dian, G., Barbey, G. and Decrox, B. (1986) *Synth. Met.*, 13, 281–89.
16. Mela, E.S. (2003) *Adv. Mater.*, 15, 481–94.
17. Ansari, R. (2006) *E-J. of Chem.*, 3, 186–201.
18. Berry, C.C. (2005) *J. Mater. Chem.*, 15, 543.
19. Kaufner, L., Cartier, R., Wustneck, R., Fichtner, I., Pietschmann, S., Bruhn, H., Schutt, D., Thunemann and A.F., Pison, U. (2007) *Nanotechnology*, 18,1.
20. Ceyhan, B., Alhorn, P., Lang, C. and Schuler, D. (2006) *N. Small*, 2, 1251.
21. Lee, C.W., Hung, K.T., Wei, P.K. and Yao, Y.D. (2006) *J. Magn. Magn. Mater.*, 304, e412.
22. Wuang, S.C., Neoh, K.G., Kang, E.T., Pack, D.W and Leckband, D.E. (2006) *Adv. Funct. Mat.*, 16, 1723.
23. Rehder, J., Rombach, P. and Hansen, O. (2001) *J. Micromech. Microeng.*, 11, 334.

24. Rangsten, P., Smith, L., Rosengren, L. and Hok, B. (1996) *Sensor Actuators A, Physical*, 52, 211.
25. Li, Z. (2002) *J. Magn. Magn. Mater.*, 252, 327.
26. Anton, I., Sabata, I.D., Vekas, L., Potencz, I. and Suciu, E. (1987) *J. Magn. Magn. Mater.*, 65, 379.
27. Meng, Z., Jibin, Z. and Jianhui, H. (2006) *J. Magn. Magn. Mater.*, 303, e428.
28. Jibin, Z., Li, X., Lu, Y. and Jianhui, M. (2002) *J. Magn. Magn. Mater.*, 252, 321.
29. Anton, I., Sabata, I.D. and Vekas, L. (1990) *J. Magn. Magn. Mater.*, 85, 219.
30. Li, D., Xu, H., He, X. and Lan, H. (2005) *J. Magn. Magn. Mater.,* 289, 399.
31. Van, W. (2006) *B. Filtration & Separation*, 43, 43.
32. Svoboda, J. (2004) *J. Phys. Separation in Science and Engineering*. 13,127.
33. Strebin, R.S., Johnson, Jr. J. W. and Robertson, D.M. (1977) *Amer. Mineralog.* 62, 374.
34. Futterer, C., Minc, N., Bormuth, V., Codarbox, J. H. and Laval, P., Rossier, J., Viovy, J. (2004) *L. Lab Chip.* 4, 351.
35. Wang, X.D., Gu, X.S., Yuan, C.W., Chen, S.J., Zhang, P.Y., Zhang, T.Y., Yao, J., Chen, F. and Chen, G. (2004) *J. Biomed. Mat. Res. Part A.* 68A, 411.
36. Schmidt, C.E., Shastri, V.R., Vacanti, J.P., Langer, R. and Proc, R. (1997) *Natl. Acad. Sci. U.S.A.*, 94, 8948.
37. Turcu, R., Bica, D.,Vekas, L., Macovel, D., Nan, A., Pana, O., Marinica, O. and Grecu, R. (2006) *C.V.L. Pop. Romanian Report in Physics*, 58, 359–67.
38. Murugendrappa, M.V., Khasim, S. and Prasad, M.V.N.A. (2005) *Bull. Mater. Sci.*, 28, 265–69.
39. Rajagopalan, S., Sawan, M., Zadeh, E.G., Savadogo, O. and Chodavarapu, V.P. (2008) Sensors 8(8), 5081–5095; doi:10.3390/s8085081
40. Gomez, N. and Schmidt, C.E. (2007) *J. Biomed. Mater*. Res. A., 81A, 135–49.
41. Gomez, N., Lee, J.Y., Nickels, J.D. and Schmidt, C.E. (2007) *Adv. Funct. Mater.*, 17, 1645–53.
42. Bajpai, A.K., Bajpai, J. and Shukla, S. (2003) *J. Mater. Sci. Mater. Med.*, 14, 347.
43. Bajpai, A K. and Kankane, S. (2007) *J. Appl. Polym. Sci*., 3, 1559–1571.
44. Bajpai, A.K. and Bundela, H. (2008) *eXpress Polym. Letters*, 2(3), 201–213.
45. Suri, K., Annapoorni, S., Tondon, R.P. (2001) *Bull. Mater. Sci.*, 24, 6, 565.
46. Bowersock, T.L., Shalaby, W.S.W., Levy, M., Blevins, W.E. White, M.R. and Borie, D.L. (1994) *J. Control Release*, 31, 245–54.
47. Kudela, V. (1988) *Encyl. Poly. Sci.Eng.*, 7, 783–807.
48. Higuchi, W.F. (1967) *J. Pharm. Sci.*, 56, 315–24.